Graphical Abstract

Challenges in studying the liquid-to-solid phase transitions of proteins using computer simulations

Beata Szała-Mendyk, Tien Minh Phan, Priyesh Mohanty, Jeetain Mittal

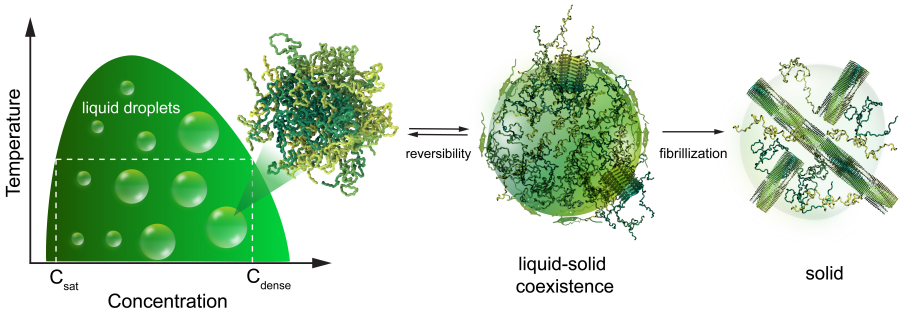

Challenges in studying the liquid-to-solid phase transitions of proteins using computer simulations

Beata Szała-Mendyk[a], Tien Minh Phan[a], Priyesh Mohanty[a], Jeetain Mittal[a,b,c,]

[a]*Artie McFerrin Department of Chemical Engineering, Texas A&M University, TAMU 3127, College Station, 77843, Texas, United States*
[b]*Department of Chemistry, Texas A&M University, TAMU 3255, College Station, 77843, Texas, United States*
[c]*Interdisciplinary Graduate Program in Genetics and Genomics, Texas A&M University, TAMU 3255, College Station, 77843, Texas, United States*

Abstract

"Membraneless organelles", also referred to as biomolecular condensates, perform a variety of cellular functions and their dysregulation is implicated in cancer and neurodegeneration. In the last two decades, liquid-liquid phase separation (LLPS) of intrinsically-disordered and multidomain proteins has emerged as a plausible mechanism underlying the formation of various biomolecular condensates. Further, the occurrence of liquid-to-solid transitions within liquid-like condensates may give rise to amyloid structures, implying a biophysical link between phase separation and protein aggregation. Despite significant advances, uncovering the microscopic details of liquid-to-solid phase transitions using experiments remains a considerable challenge and presents an exciting opportunity for the development of computational models which provide valuable, complementary insights into the underlying phenomenon. In this review, we highlight recent biophysical studies which provide new insights into the molecular mechanisms underlying liquid-to-solid (fibril) phase transitions of folded, disordered and multi-domain proteins. Next, we summarize the range of computational models used to study protein aggregation and phase separation. Finally, we discuss recent computational approaches which attempt to capture the underlying physics of liquid-to-solid transitions along with their merits and shortcomings.

Keywords:
Amyloid fibrils, liquid-liquid phase separation (LLPS), liquid-to-solid transition (LST), molecular dynamics (MD) simulation

Introduction

A hallmark of several neurodegenerative diseases is the appearance of cytoplasmic inclusions in brain and spinal cord tissues which are comprised of insoluble protein aggregates which may be amorphous or amyloid in nature [1]. The pathological aggregation of folded (e.g., SOD1), intrinsically disordered (e.g., Tau, α-synuclein) and multidomain proteins (e.g. TDP-43, FUS, hnRNPs) is associated with degenerative diseases such as Alzheimer's disease, Parkinson's, disease, amyotropic lateral sclerosis (ALS) and fronto-temporal dementia (FTD). In the last decade, these proteins were also shown to undergo liquid-liquid phase separation (LLPS) *in vitro* [2] and are implicated in the assembly and regulation of various "membraneless" organelles or biomolecular condensates [3]. While many of these condensates appear to exhibit liquid-like properties, some form gel-like structures while others form solid-like (amyloid) structures [4]. *In vitro* studies indicated that longer timescale incubation of liquid droplets formed by disordered proteins can promote the formation of amyloid aggregates under physiological conditions, implying a potential link between LLPS and pathological aggregation as discussed in previous reviews [5, 6]. Liquid condensates may therefore serve as attractive targets for the development of potential therapeutics for neurodegenerative diseases [7, 8].

Email addresses: bszalamendyk@tamu.edu (Beata Szała-Mendyk), tienminhphan@tamu.edu (Tien Minh Phan), priyeshm@tamu.edu (Priyesh Mohanty), jeetain@tamu.edu (Jeetain Mittal)

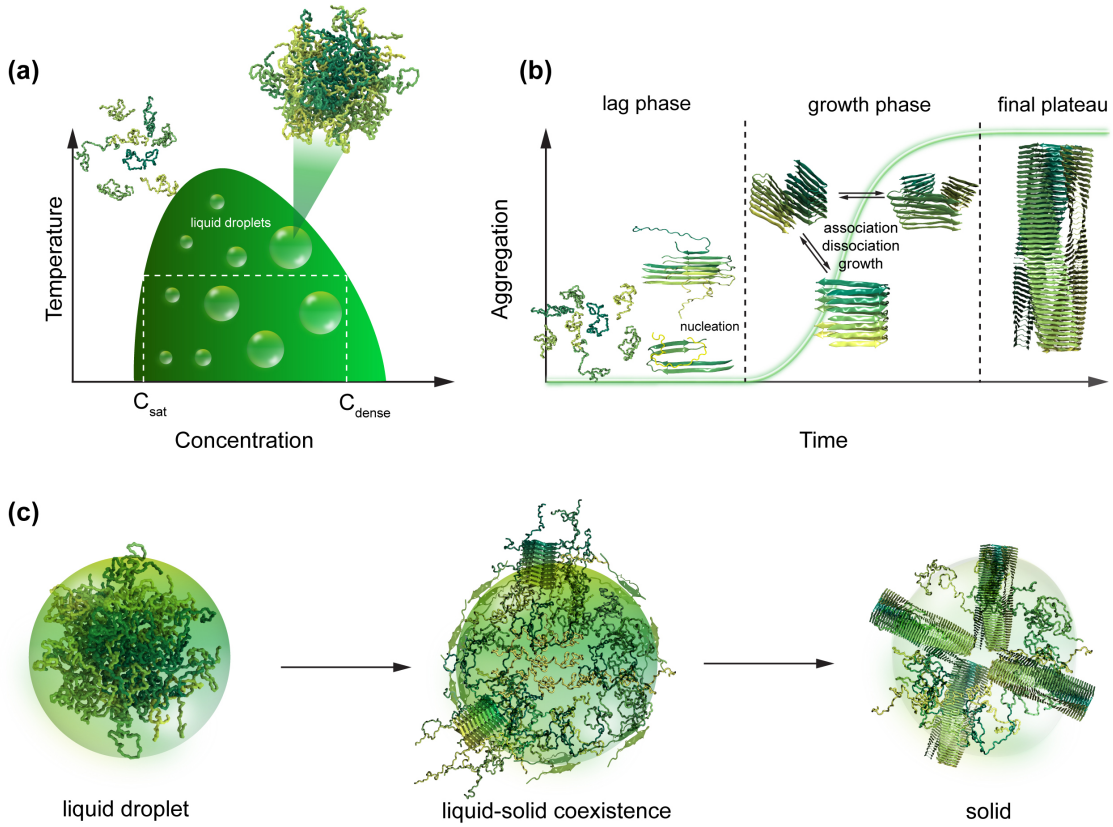

Figure 1: Relationship between LLPS and fibril fromation. **(a)** At a given temperature, liquid-liquid phase separation is delineated by a coexistence curve or binodal. Phase separation of any concentration above the saturation concentration (C_{sat}) manifests as liquid droplets with a higher concentration (C_{dense}). **(b)** Protein aggregation typically shows a sigmoidal curve of growth kinetics, where two relatively flat regions (lag phase and plateau phase, respectively) are connected by a steep transition zone (growth phase). In the lag phase, partially folded proteins associate to form primary nuclei. As nuclei reach the critical size, small fibrils emerge and elongate (the growth phase). Secondary processes, such as lateral growth, association, and dissociation of unmatured fibrils, also occur in this phase. When the monomer concentration reaches equilibrium, the system enters the plateau phase. **(c)** A liquid-to-solid transition (LST) occurs during droplet maturation with the emergence of hydrophobic cores forming from catalytic activities on the droplet interface. The fibril structures were generated using the CreateFibril tool [11].

Factors governing liquid-to-solid transitions based on recent biophysical experiments

LLPS involves demixing of a homogeneous macromolecular solution which gives rise to two distinct phases, a dilute and dense phase, often represented in the form of a coexistence curve (Fig. 1a). Amyloid formation may occur independent of phase separation (Fig. 1b) through the formation of an initial nucleus (lag phase) which undergoes elongation to form fibrils (growth phase). Maturation of liquid condensates results in a slowdown of internal dynamics to eventually form gel-like and/or fibrillar (amyloid) assemblies (Fig. 1c). While the liquid phase is maintained by a variety of weak interactions [9] , amyloid fibrils adopt a characteristic cross-β structure which is stabilized by polar and hydrophobic interactions [10]. Post-translational modifications [12] (e.g., acetylation, phosphorylation) and pathogenic mutations [13] were shown to modulate the liquid-like nature of condensates both *in vitro* and *in vivo*. *In vitro* studies indicate that LLPS can promote amyloid formation of disordered regions in proteins associated with neurodegeneration [5, 14, 15]. Biophysical techniques such as NMR spectroscopy and fluorescence-based methods have been extensively utilized to provide insights into the conformational dynamics and residue-level interactions associated with the condensed phase [16, 17]. More recently, such methods were employed to obtain insights into the underlying, molecular mechanisms of liquid-to-solid transition (LST).

LLPS is often associated with conformational transitions of folded, disordered and multidomain proteins [18, 19, 20]. Sequence-dependent conformational transitions regulate intermolecular interactions which are critical to LLPS and therefore, may also provide clues regarding the mechanisms underlying LST. Ray et al. identified domain-level interactions which drive LST of α-synuclein [21]**. Based on solution NMR and FRET experiments, they observed that both N-terminal (aa:1-

60) and hydrophobic NAC (aa:61-95) domains contributed towards intermolecular interations which promote LST and give rise to amyloid fibrils. Cross-linking mass spectroscopy (XL-MS) experiments indicate that the conformational ensemble of α-synuclein undergoes a population shift during LLPS from compact "hairpin-like" conformations stabilized by complementary N/C-terminal electrostatic interactions towards more expanded conformations [22]. Along these lines, truncated C-terminal variants (aa:1-115/122) showed enhanced LLPS and amyloid aggregation, establishing the inhibitory effect of the N/C-terminal intramolecular interactions on the phase separation of α-synuclein [23]. Solution and solid state NMR experiments indicate that LLPS-mediated amyloid formation of α-synuclein proceeds through the formation of oligomeric intermediates which comprise of both unstructured and β-rich ensembles [24].

Wen et al. studied the conformational changes of full-length Tau (441 aa) which were associated with its LLPS-dependent amyloid formation [25]. Utilizing several fluorescence-based methods (smFRET, FCS and anisotropy), they observed that Tau underwent conformational expansion and formed nanoclusters within the crowded droplet environment even at subnanomolar concentrations. The expansion of Tau involved extension of N/C-terminal regions and resulted in exposure of the microtubule-binding region (MTBR) which is crucial for fibrillation. LSTs may be controlled by metal co-factors which stabilize the folded state of a protein. Das et al. showed that liquid droplets of partially-disordered, SOD1 wild type which formed upon removal of its metal co-factor - Zinc, underwent a liquid-to-solid transition giving rise to amyloid fibrils (within 3 days) [26]. While LLPS of SOD1 was reversible upon addition of Zn, the stability of amyloid fibrils were unaffected. Further, it was observed the liquid droplets formed by severe ALS mutants (G85R/I113T) of SOD1 which were deficient in Zn-binding also gave rise to amyloid fibrils.

The intrinsically disordered, low complexity domains (LCD) of several RNA binding proteins (e.g., TDP-43, FUS and hnRPNA1/2) were shown to undergo phase separation and maturation into fibril-like structures [27]. The phase separation of TDP-43 C-terminal LCD (aa:267-414) is dependent upon interactions mediated through the conserved helical region (CR, aa:319-341) along with several aromatic residues in the CR-flanking, intrinsically disordered regions (IDR1/2) [28, 29, 30]. Pantoja-Uceda et al. studied the liquid-to-amyloid transition of TDP-43 LCD under low pH conditions (without salt or RNA) and uncovered the distinct roles of LCD regions in LST [31]*. Using fluorescence-based confocal microscopy, it was observed that fibril formation initiated at the droplet interface. Real time NMR experiments indicated that CR was more critical than FG motifs in IDR1/2 for initiation of LLPS. In contrast, solid state (SS) NMR analysis of LLPS-derived fibrils coupled with cross-seeding experiments established that in addition to CR, fibrillation was also dependent on six phenylalanine residues in IDR1/2. Using SS NMR experiments, Fonda et al. [32] identified an additional fibril-forming core in IDR2 (aa:365-400) which counteracts the ability of CR to undergo fibrillation within condensates. These observations highlight the mechanistic complexity of LLPS-derived fibrillation which arises through competing interactions between LCD segments.

The crowded environment within the droplet can influence the structure of fibrils formed through dynamic protein-protein interactions. Using solid-state MAS (Magic Angle Spinning) NMR spectroscopy, Berkeley et al observed that wild type FUS LCD (aa:1-163) remained predominantly in a gel-like state (even upto 30 days) while G156E mutant readily converted to an amyloid-state (within 5 days) [33]*. The overall structure of the amyloid species formed by both FUS LC wild type and G156E were similar. Interestingly, several residues were not part of the β-sheet rich amyloid core (aa:39-95) observed in seeded fibrils, implying a modification of the fibril structure within the droplet environment.

Alterations in physical parameters (e.g., shear stress, temperature) may exert a significant influence on the kinetics of liquid-to-solid transitions for disordered proteins. Shen et al. demonstrated that the application of shear stress values in the physiological range using microfluidics could induce LST (fibrillation) in condensates formed by multidomain proteins [34]**. Based on these observations, the authors proposed a model for shear-induced fibrillation wherein shear aligns polypeptide chains within droplet leading to the formation of β-sheet structures. Chatterjee et al. observed that FUS LCD (aa:1-163) could form kinetically trapped condensates (KTCs) upon cooling (4^{o} C) which showed arrested coalescence and higher β-sheet content compared to condensates formed at room temperature [35]. Further, KTCs could reconvert into untrapped, liquid-like condensates by thermal annealing.

Aggregation-prone proteins (e.g., α-synuclein, Tau and prion) can form complex coacervates (heterotypic condensates) through complementary, domain-specific electrostatic interactions which convert over time to amyloid co-aggregates.[36, 37, 38]. Based on time-resolved experiments, Mukopadhyay and co-workers [37, 38] observed that heterotypic condensates of

prion/α-synuclein and prion/tau formed transient electrostatic nanoclusters on the nanosecond timescale. At longer timescales (>40 hours), the complex coacervates underwent conformational rearrangements to form amyloid co-aggregates. Gracia et al. [36] observed that only liquid-like coacervates (unsatisfied valences) of α-synuclein/Tau could coalesce to form larger droplets and give rise to amyloid-like aggregates in the droplet interior through rearrangement of protein interaction networks. In contrast, droplets which underwent gelation remained small in size (due to satisfied valences) and were unable to form aggregates.

Protein-RNA interactions can modulate LSTs of RNA-binding proteins (RBPs) which are associated with neurodegenerative diseases. Depending on their concentration, length, sequence and secondary structural properties, RNA molecules may either promote or inhibit LSTs [39]. While *in vitro* experiments performed at low RNA concentrations promote LLPS of RBPs, the presence of excess RNA (physiological concentrations) generally inhibits their phase separation and subsequent aggregation both *in vitro* and *in vivo*. Interestingly, Ishiguro et al. showed that interactions with G-quadruplex (structured) RNA enhanced LLPS and LST of FUS full-length [40]. The interaction of RNA-free (unbound) RBPs with chaperones suppresses their LSTs both *in vitro* and *in vivo*. For example, the interaction of FUS LCD (aa:1-163) with Hsp27 chaperones (phosphorylated form) could inhibit its LLPS and LST [41]. Similarly, interactions between TDP-43 LCD and Hsp70 chaperones promoted the formation of intranuclear condensates and inhibited TDP-43 aggregation [42, 43, 44].

Biomolecular condensates can influence protein aggregation by affecting the partioning (condensate interface or interior) of amyloid-prone proteins. Differential localization of these proteins within condensates can affect their stability and reactivity with other macromolecules and metabolites. Küffner et al. showed that the recruitment of aggregation-prone Aβ-42 fragment into LCD condensates of DEAD-box proteins (LAF-1, Dbp1 and Ddx4) could inhibit amyloid formation through competing heterotypic interactions [45]. Lipiński et al. utilized three complex coacervate systems (formed from charged peptides, RNA or ATP) and showed that aggregation of α-synuclein could be accelerated when it localized to the condensate interface compared to the interior [46]*.

In summary, a complex interplay between sequence-dependent interactions (homotypic and heterotypic) and physical parameters (e.g., temperature, pH, salt, metabolites) govern the overall conformational dynamics underlying LLPS-dependent fibrillation.

All-atom models for studying phase separation and aggregation

Complementary to experiments, molecular simulations have been successfully utilized to provide high resolution insights into protein dynamics and assembly. redAlthough atomistic simulations are unable to directly probe LLPS and aggregation processes for many IDPs due to length and timescale limitations, they can be useful for the investigation of single-chain properties such as intramolecular interactions, secondary structure and conformational changes associated with LLPS [28, 30, 47]. Back mapping of coarse-grained (CG) models to an all-atom representation allows for investigating various interaction modes in intrinsically disordered domains, e.g., cation–π, sp^2/π, hydrogen bonding, and salt-bridge, that cannot be resolved in CG models [48, 49] (Fig. 2a). All-atom simulations were used to characterize intermolecular interactions implicated in the phase separation of short disordered fragments [50] and domains [48]** (Fig. 2a, 3a). With regard to protein aggregation, all-atom simulations were recently used to study the formation of Aβ dimers in solution and a neuronal membrane model [51] to explain the mechanism of oligomer-mediated neuronal toxicity. Additional examples of studies utilizing atomistic simulations to study LLPS and aggregation are discussed in recent reviews [16, 52].

Coarse-grained models for studying phase separation and aggregation

Coarse-grained models wherein entire macromolecules (e.g. protein, RNA) are represented by one or a few particles, can be useful in identifying the key forces driving phase separation at high computational efficiency. CG models can bridge the timescale gap between simulation and experiment by selectively retaining fewer degrees of freedom compared to more expensive, atomistic models. CG approaches provide a transferable framework to compute protein phase diagrams in temperature - concentration space, which can be compared to experimental phase behavior.

The HPS model developed in our group, combines electrostatic and short-range interactions parametrized based on the hydrophobicity scale of Kapcha and Rossky [53], has been widely used to study the sequence-dependent phase separation of several IDPs. The model was further extended to incorporate temperature-dependent effects, account for post-translational modifications, salt-dependent behavior and capture the multicomponent phase behavior of IDP/polynucleotide mixtures [54, 55, 56, 57, 58]. Caveats associated with the HPS model include overprediction of R_g for many IDPs and failure to capture the effect of arginine-to-lysine or tyrosine-to-phenylalanine substitutions observed in experiments [59, 60]. Attempts have been made to improve the HPS model by re-parametrizing short-ranged interactions based on the force balance or Bayesian parameter learning methods or the Urry hydropathy scale, or using maximum entropy optimization based on SAXS data [59, 61, 62, 63]. More recently, other CG strategies have been applied to study the dominant contributions of π-related interactions on LLPS propensities of IDPs [60, 64], role of LLPS in dipeptide repeat protein (DPR) toxicity [65], mechanism of ATP-dependent modulation of FUS phase separation [66] and phase separation of peptide/protein-RNA systems. [58, 67, 68].

The CG framework has also been applied to study the phase separation of multidomain proteins comprising both folded and disordered domains [69, 70]. Further, a reparameterized variant of the HPS model [60] along with the compatible RNA model [58] was used to study the influence of RNA concentration and length on the transport properties and stability of condensates formed by RNA-binding proteins such as TDP-43, FUS and hnRNPA1 [71]. Higher resolution models can also be used with explicit solvent; for instance, Benayad et al. scaled nonbonded interactions in the MARTINI model (version 2.2) (two to four heavy atoms per residue) to simulate liquid droplet formation of FUS-LC and characterize its material properties from the underlying protein dynamics [72]. A reparameterization of the MARTINI model (version 3.0) with improved interaction balance, has been used to investigate ion and nucleotide partitioning between poly-lysine/poly-glutamate coacervates and the surrounding solvent [73]. Despite the simplicity of CG models, they have been utilized with great success in uncovering mechansitic insights into formation of biomolecular condensates. However, it is still challenging for CG models to accurately reproduce experimental results or capture local secondary structure and their effects on the phase-separation propensities of

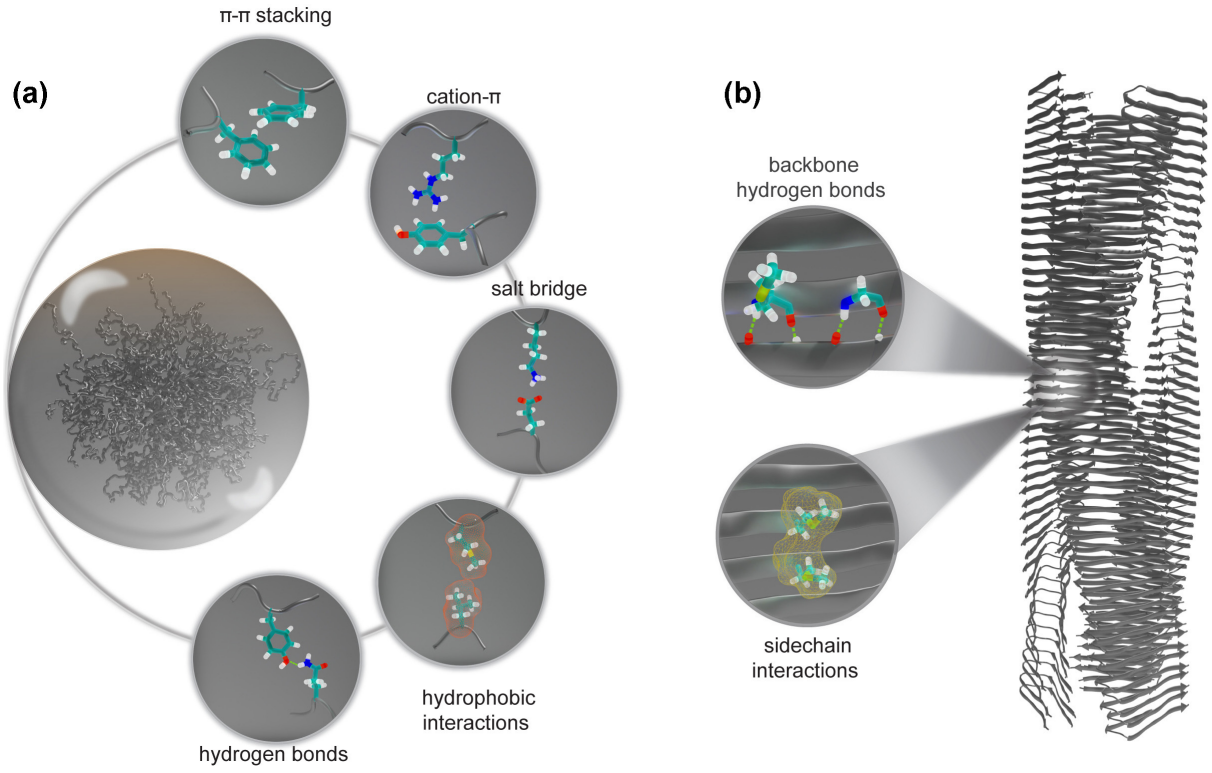

Figure 2: Interaction modes contribute to protein phase separation and protein aggregation. **(a)** Liquid-liquid phase separation is stabilized by various intermolecular interactions, including $\pi - \pi$ stacking, cation-π, salt bridges, hydrophobic interactions, and hydrogen bonds. **(b)** In amyloidogenic aggregation, backbone hydrogen bonds are essential for maintaining the secondary and tertiary structures of proteins and protein-protein interactions. Additionally, side-chain interactions involving different interaction modes can further enable the formation of hydrophobic cores, stabilize the structure of the protein and facilitate protein aggregation.

IDPs. Further experimental advancements will provide exciting opportunities for the development of accurate and efficient CG models for studying biological phase separation.

CG models to study protein aggregation range from highly coarse to near atomistic in terms of model resolution [74]. Such a hierarchical approach greatly reduces the computational cost associated with simulation of the aggregation pathway at the expense of lower model resolution. (Fig. 3c). Studies utilizing phenomenological models indicated that the β-propensity [75], hydrophobicity [76], hydrophobic patterning [77], chain stiffness [77, 78], and side-chain geometry [79] are critical factors for fibrillation. The fibril elongation mechanism ("dock-lock") of an Amyloid-β fragment was studied using a CG model (UNRES), revealing the intra-monomer hairpin as a structural intermediate [80]. The higher fibril forming propensity of FUS LCD core 1 (aa:$39-95$) compared to core-2 (aa:112-150) was investigated using a single-bead per residue CG model developed for IDPs [81]. CG simulations indicated a higher population of excited states corresponding to the core-1 fibril topology in the monomeric ensemble, highlighting the role of sequence-specific enthalpic effects in determining fibrillation pathways. Knowledge-based CG models were recently utilized to design *de novo* peptides which form β-rich nanofibers [82, 83]*. The coarsest models represent the whole peptide or protein as a single unit with a tunable interaction potential which controls the transition between protein states. Despite their lower resolution, highly simplified models can simulate systems containing hundreds of proteins, which makes them especially useful for kinetic studies and quantitative comparison with experiments [84, 85].

Computational approaches for studying liquid-to-solid transitions

Recent attempts at modeling LSTs of proteins have utilized phenomenological approaches to circumvent the timescale limitations associated with unbiased CG methods. Such approaches typically involve a CG description of peptides and proteins (residue or domain-level) coupled with either modifications to the potential energy function or the incorporation of user-defined criteria to drive the formation of ordered, fibril-like structures within the liquid phase.

Xing et al. [91]* studied the liquid-to-solid transition for a model CG peptide using discrete molecular dynamics (DMD) simulations. The peptide model was allowed to adopt two low energy states: fibrillation incompetent (helical or random coil conformations) and fibrillation competent (β-sheet) states. It was observed that fibrillation via LLPS proceeded through the formation of a high-density liquid phase (HDLP) comprising of either stable or transient oligomers in a concentration-dependent manner. More recently, the authors utilized the same methodology to analyze length-dependent effects of flanking polar sequences on the structure of oligomers formed by the model peptide en route to fibrillation [95].

CG simulations of FUS full-length condensates revealed that the interplay between homo and hetero-domain interactions controls condensate morphology [90]. The strength of interdomain interactions were tuned by modifying the ε parameter (energy well depth) of the Lennard-Jones potential based on the known roles of FUS domains in promoting either LLPS or fibrillation. Depending on the relative strength of homo and heterotypic interactions involving prion-like and RNA-binding domains, condensate morphologies varied from disordered, well-mixed assemblies to ordered, fibrillar assemblies with a core-shell structure.

Garaizar et al. studied the maturation of FUS liquid condensates into gel-like structures using a minimal CG model (domain-level) coupled with a dynamical algorithm which irreversibly forms inter-chain β-sheets with time [96]. Briefly, the relative interaction strengths between aggregation-prone, FUS peptides in the disordered and ordered (fibril) states were inferred from all-atom simulations, incorporated into residue-level CG simulations to assess their impact on the structural organization of condensates and subsequently utilized to develop a minimal CG model. The non-equilibrium, dynamical algorithm was also used in combination with a residue-level CG model to study the effect of RNA concentration on the time-dependent formation of inter-protein β-sheets within FUS and hnRNAP1 condensates [88]*. It was observed that the recruitment of high concentrations of RNA into condensates decelerates the accumulation of β-sheets through a combination of attractive RNA-protein interactions and repulsive RNA-RNA interactions.

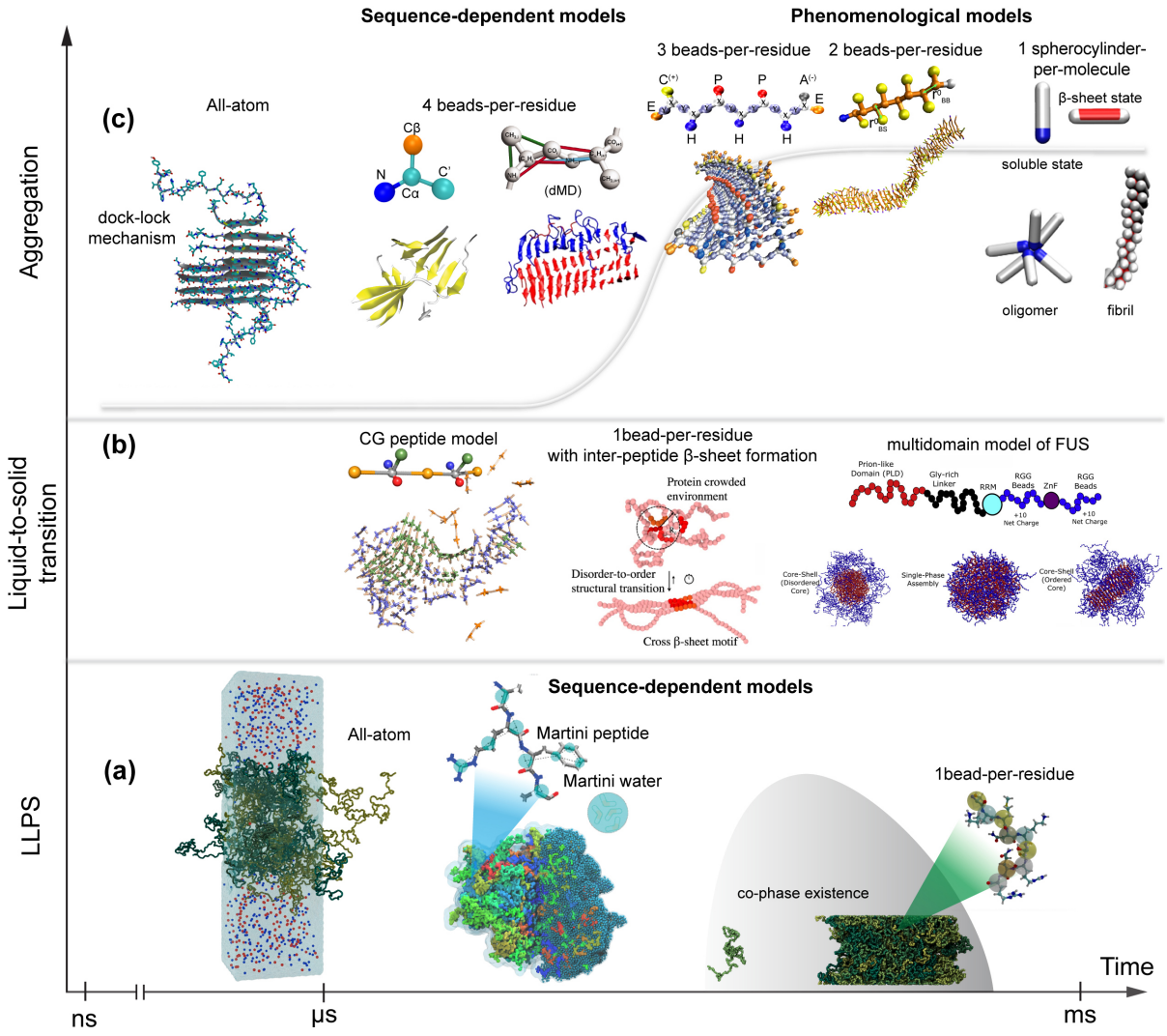

Figure 3: Computational models for the study of protein phase separation, protein aggregation, and liquid-to-solid- transition at various time scales and model resolutions. **(a)** AA slab simulation was utilized to explore interaction modes, and CG simulations using a re-balanced Martini model were employed to study dynamic materials properties of proteins within the condensed phase. CG slab simulations using a sequence-dependent one-bead-per-residue model were applied to establish one-phase and two-phase regimes of the phase diagram. **(b)** Recent computational work on liquid-to-solid transition: a phenomenological CG peptide model was used to study general properties of LLPS and amyloid aggregation, a one-bead-per-residue CG model with inter-peptide β-sheet formation was applied to explore the role of RNA on the aging of biomolecular condensate, and a CG multidomain model was developed to explore structural properties within FUS condensate. **(c)** Different model resolutions were employed to study different phases of amyloid aggregation ranging from explicit solvent atomistic simulation to sequence-dependent near atomic four-bead-per-residue models, to phenomenological models with coarser graining varying from three- and two-bead-per-residue to one-bead-per-protein. It should be noted that the CG models used to study fibril formation can also be used to study the early stages of protein aggregation such as intramolecular conformational changes and nucleation events [81, 86]. Images of computational models were adapted with permission under the Creative Commons Attribution License (CC BY 4.0) [72, 87, 79, 88], Creative Commons Attribution License (CC BY 3.0) [89], Copyright 2022 Biophysical Society [90], Copyright 2020 American Chemical Society [91], Copyright 2010 Wiley-Liss, Inc. [92], and under AIP Publishing [93, 75, 94].

Challenges and Future Outlook

Growing evidence suggests that physiological, liquid-like condensates may transform into pathological aggregates, including highly-ordered, amyloid fibrils. Various experimental techniques have been recently employed to investigate the intrinsic (e.g. sequence, secondary structure) and extrinsic (pH, salt concentration, crowding, etc.) factors that control LST of protein condensates. However, additional high resolution are required to gain new insights into the sequence determinants of protein aggregation within the condensed phase [97]. Given their past success in studying LLPS and aggregation independently, computer simulations are beginning to serve as a powerful tool to explore the underlying physics which links these two phenomena.

The large computational expense associated with atomistic models has led to studies utilizing phenomenological approaches (domain-level or residue-level resolution) which explicitly incorporate system-specific biases based on experimental information to drive LST. Although these models are able to reproduce the experimental trends, the system-specific nature of these models prevents them from providing a more general view of the underlying process. Moreover, such models require caution when choosing system features to be incorporated into the CG representation and handling inconsistencies associated with experiments.

For one-bead-per-residue CG models, difficulties in modeling inter-protein β-sheets also arises from the lack of explicit separation between the backbone and side-chain interactions. Backbone-mediated interactions are generic to all proteins, including backbone-backbone hydrogen bonds which stabilize fibrils. On the other hand, the identity of side chains differentiate proteins, contributing to fibril polymorphisms and altering LLPS tendency [9]. To overcome this, one can add additional beads per residue or apply special anisotropic potentials [98] which however, comes at an increased computational cost.

To gain a more general view of LST, future models need to describe the sequence-specific secondary structure propensities of amino acids. The incorporation of a conformation-dependent term into a one-bead-per-residue model led to the emergence of internal order within liquid droplets [99]. Recently, the HPS CG model has been modified (HPS-SS) to include a sequence-dependent, dihedral potential term in order to reproduce the variable helical propensity for amino acids [100]*. Explicit modeling of helix-to-coil transitions enables CG simulations to investigate the role of helix-helix interactions in LLPS and aggregation. Future efforts aimed at extending the scope of the HPS-SS model to accurately describe extended-β conformations can allow for modeling the formation of inter-protein β-sheets within condensates.

In summary, recent computational approaches using CG models enable an efficient exploration of the conformational landscape underlying LST of disordered and multi-domain proteins, albeit at the expense of low model resolution and preimposed structural biases. However, moving forward, there is a need for structurally-unbiased CG models which capture the sequence-dependent structural propensities of amino acids and thereby enable a more accurate description of the conformational transitions and inter-molecular interactions associated with LST.

Acknowledgement

Our research on biomolecular phase separation is supported by the National Institutes of Health Grants R01NS116176, R01GM136917, the National Science Foundation Grant DMR2004796, and the Welch Foundation Grant A-2113-20220331.

References

[1] C.A. Ross and M.A. Poirier. What is the role of protein aggregation in neurodegeneration? *Nat. Rev. Mol. Cell Biol.*, 6:891–898, 2005.

[2] P. Mohanty, U. U. Kapoor, Sundaravadivelu Devarajan D., T.M. Phan, A. Rizuan, and J. Mittal. Principles governing the phase separation of multidomain proteins. *Biochemistry*, 61:2443–2455, 2022.

[3] S. Alberti and A.A. Hyman. Biomolecular condensates at the nexus of cellular stress, protein aggregation disease and ageing. *Nat. Rev. Mol. Cell Biol.*, 22:196–213, 2021.

[4] Y. Shin and C.P. Brangwynne. Liquid phase condensation in cell physiology and disease. *Science*, 357:eaaf4382, 2017.

[5] W. M. Babinchak and W. K. Surewicz. Liquid-liquid phase separation and its mechanistic role in pathological protein aggregation. *J. Mol. Biol.*, 432:1910–1925, 2020.

[6] A. Zbinden, M. Pérez-Berlanga, P. De Rossi, and M. Polymenidou. Phase separation and neurodegenerative diseases: A disturbance in the force. *Dev. Cell.*, 55:45–68, 2020.

[7] M. Biesaga, M. Frigolé-Vivas, and X. Salvatella. Intrinsically disordered proteins and biomolecular condensates as drug targets. *Curr. Opin. Chem. Biol.*, 62:90–100, 2021.

[8] D.M. Mitrea, M. Mittasch, B.F. Gomes, I.A. Klein, and M.A. Murcko. Modulating biomolecular condensates: a novel approach to drug discovery. *Nat. Rev. Drug Discov.*, 21:841–862, 2022.

[9] G.L. Dignon, R.B. Best, and J. Mittal. Biomolecular phase separation: From molecular driving forces to macroscopic properties. *Annu. Rev. Phys. Chem.*, 71:53–75, 2020.

[10] R. Gallardo, N. A. Ranson, and S. E. Radford. Amyloid structures: much more than just a cross-β fold. *Curr. Opin. Struct. Biol.*, 60:7–16, 2020.

[11] M. R. Smaoui, F. Poitevin, M. Delarue, P. Koehl, H. Orland, and J. Waldisp uhl. Computational assembly of polymorphic amyloid fibrils reveals stable aggregates. *Biophys. J.*, 104:683–693, 2013.

[12] M. Hofweber and D. Dormann. Friend or foe-post-translational modifications as regulators of phase separation and RNP granule dynamics. *J. Biol. Chem.*, 294:7137—-7150, 2019.

[13] B. Tsang, I. Pritišanac, S.W. Scherer, A.M. Moses, and J.D. Forman-Kay. Phase separation as a missing mechanism for interpretation of disease mutations. *Cell*, 183:1742—1756, 2020.

[14] T. R. Peskett, F. Rau, J. O'Driscoll, R. Patani, A. R. Lowe, and H. R. Saibil. A liquid to solid phase transition underlying pathological huntingtin exon1 aggregation. *Mol. Cell*, 70:588–601, 2018.

[15] X. Gui, S. Feng, Z. Li, Y. Li, B. Reif, B. Shi, and Z. Niu. Liquid–liquid phase separation of amyloid-β oligomers modulates amyloid fibrils formation. *J. Biol. Chem.*, 299:102926, 2023.

[16] N.L. Fawzi, S.H. Parekh, and J. Mittal. Biophysical studies of phase separation integrating experimental and computational methods. *Curr. Opin. Struct. Biol.*, 70:78–86, 2021.

[17] A. Abyzov, M. Blackledge, and M. Zweckstetter. Conformational dynamics of intrinsically disordered proteins regulate biomolecular condensate chemistry. *Chem. Rev.*, 122(6):6719–6748, 2022.

[18] P. Yang, C. Mathieu, R.M. Kolaitis, P. Zhang, J. Messing, U. Yurtsever, Z. Yang, J. Wu, Y. Li, Q. Pan, J. Yu, E. W. Martin, T. Mittag, H.J. Kim, and J. P. Taylor. G3bp1 is a tunable switch that triggers phase separation to assemble stress granules. *Cell*, 181:321–345, 2020.

[19] E. W. Martin, T. S. Harmon, J. B. Hopkins, S. Chakravarthy, J. J. Incicco, P. Schuck, A. Soranno, and T. Mittag. A multi-step nucleation process determines the kinetics of prion-like domain phase separation. *Nature Communications*, 12:1–12, 2021.

[20] K.M. Ruff, Y.H. Choi, D. Cox, A.R. Ormsby, Y. Myung, D.B. Ascher, S.E. Radford, R. V. Pappu, and D.M. Hatters. Sequence grammar underlying the unfolding and phase separation of globular proteins. *Mol. Cell.*, 82:3193–3208.e8., 2022.

[21] S. Ray, N. Singh, R. Kumar, K. Patel, S. Pandey, D. Datta, J. Mahato, R. Panigrahi, A. Navalkar, S. Mehra, L. Gadhe, D. Chatterjee, A. S. Sawner, S. Maiti, S. Bhatia, J. A. Gerez, A. Chowdhury, A. Kumar, R. Padinhateeri, R. Riek, G. Krishnamoorthy, and Samir K. Maji. α-Synuclein aggregation nucleates through liquid–liquid phase separation. *Nature Chemistry*, 12:705–716, 2020.
$\star\star$ This study presents detailed insights into LLPS and LLPS-dependent amyloid formation of α-Synuclein based on in vitro experiments and a cellular model. Using a variety of biophysical techniques, it was established that interactions involving N-terminal (aa:1-60) and hydrophobic NAC (aa:61-95) domains promoted LLPS-mediated amyloid formation. LLPS was also demonstrated in cells wherein α-Synuclein droplets eventually transformed into perinuclear aggresomes and regulated by microtubules.

[22] D. Ubbiali, M. Fratini, L. Piersimoni, C. H. Ihling, M. Kipping, I. Heilmann, C. Iacobucci, and A. Sinz. Direct observation of "elongated" conformational states in α-synuclein upon liquid-liquid phase separation. *Angewandte Chemie*, 134:1–6, 2022.

[23] S. Huang, X. Mo, J. Wang, X. Ye, H. Yu, and Y. Liu. α-synuclein phase separation and amyloid aggregation are modulated by c-terminal truncations. *FEBS Letters*, 596:1388–1400, 2022.

[24] M. Takamuku, T. Sugishita, H. Tamaki, L. Dong, M. So, T. Fujiwara, and Y. Matsuki. Evolution of α-synuclein conformation ensemble toward amyloid fibril via liquid-liquid phase separation (llps) as investigated by dynamic nuclear polarization-enhanced solid-state mas nmr. *Neurochemistry International*, 157:105345, 2022.

[25] J. Wen, L. Hong, G. Krainer, Q.-Q. Yao, T.P.J. Knowles, S. Wu, and S. Perrett. Conformational expansion of Tau in condensates promotes irreversible aggregation. *J. Am. Chem. Soc.*, 143:13056—-13064, 2021.

[26] B. Das, S. Roychowdhury, P. Mohanty, A. Rizuan, J. Chakraborty, J. Mittal, and K. Chattopadhyay. A Zn-dependent structural transition of SOD1 modulates its ability to undergo phase separation. *EMBO J.*, 42:1–20, 2023.

[27] J. H. Wiedner and J. Giudice. It's not just a phase: function and characteristics of rna-binding proteins in phase separation. *Nat. Struct. Mol. Biol.*, 28:465–473, 2021.

[28] A.E. Conicella, G.H. Zerze, J. Mittal, and N.L. Fawzi. ALS mutations disrupt phase separation mediated by α-helical structure in the TDP-43 low-complexity C-terminal domain. *Structure*, 24:1537—-1549, 2016.

[29] H. B. Schmidt, A. Barreau, and R. Rohatgi. Phase separation-deficient tdp43 remains functional in splicing. *Nat. Commun.*, 10:4890, 2019.

[30] A. E. Conicella, G. L. Dignon, G. H. Zerze, H. B. Schmidt, A. M. D'Ordine, Y. C. Kim, R. Rohatgi, Y. M. Ayala, J. Mittal, and N. L. Fawzi. TDP-43 α-helical structure tunes liquid–liquid phase separation and function. *Proc. Natl. Acad. Sci. U.S.A.*, 117(11):5883–5894, 2020.

[31] D. Pantoja-Uceda, C. Stuani, D. V. Laurents, A.E. McDermott, E. Buratti, and M. Mompeán. Phe-Gly motifs drive fibrillization of TDP-43's prion-like domain condensates. *PLOS Biol.*, 19:e3001198, 2021.
$\star$ The dynamics of liquid-to-amyloid transition of TDP-43 C-terminal domain (CTD) was studied using in vitro microscopy and NMR-based methods under low pH conditions without salt. The study provides rich, mechanistic insights into the site of fibrillation in liquid droplets (i.e., the droplet interface) along with the underlying cooperativity between the CR and IDR regions during LLPS and subsequent aggregation of CTD.

[32] B. D. Fonda, K. M. Jami, N. R. Boulos, and D. T. Murray. Identification of the rigid core for aged liquid droplets of an RNA-binding protein low complexity domain. *J. Am. Chem. Soc.*, 143(17):6657–6668, 2021.

[33] R.F. Berkeley, M. Kashefi, and G.T. Debelouchina. Real-time observation of structure and dynamics during the liquid-to-solid transition of FUS LC. *Biophys. J.*, 120:1276—1287, 2021.
$\star$ This study reports on the differences in kinetics of liquid-to-solid transition for FUS LCD wild type and a pathogenic mutant - G156E using solid state NMR methods. FUS LCD wild type condensate remained predominantly in a gel-like state (upto 30 days) while the mutant condensate rapidly converted to fibrils (within 7 days). Further, the structure of the fibril core formed under LLPS conditions differed from seeded fibrils. These findings imply that fibril morphology can be shaped by dynamic protein-protein interactions within the droplet phase.

[34] Y. Shen, F.S. Ruggeri, D. Vigolo, A. Kamada, S. Qamar, A. Levin, C. Iserman, S. Alberti, P.S. George-Hyslop, and T.P.J. Knowles. Biomolecular condensates undergo a generic shear-mediated liquid-to-solid transition. *Nat. Nanotechnol.*, 15:841–847, 2020.
$\star\star$ The study demonstrates that the microfluidic application of physiological shear stress values could induce LST (fibrillation) in condensates formed by multidomain proteins. A model for shear-induced LST was proposed wherein the application of shear aligns polypeptide chains within droplets to promote intermolecular interactions which lead to the formation of β-sheet structures.

[35] S. Chatterjee, Y. Kan, M. Brzezinski, K. Koynov, R.M. Regy, A.C. Murthy, K.A. Burke, J.J. Michels, J. Mittal, N.L. Fawzi, and S.H. Parekh. Reversible kinetic trapping of FUS biomolecular condensates. *Adv. Sci.*, 9:2104247, 2022.

[36] P. Gracia, D. Polanco, J. Tarancón-Díez, I. Serra, M. Bracci, J. Oroz, D. V. Laurents, I. García, and N. Cremades. Molecular mechanism for the synchronized electrostatic coacervation and co-aggregation of α-synuclein and tau. *Nature Communications*, 13:4586, 2022.

[37] A. Agarwal, L. Arora, S. K. Rai, A. Avni, and S. Mukhopadhyay. Spatiotemporal modulations in heterotypic condensates of prion and α-synuclein control phase transitions and amyloid conversion. *Nature Communications*, 13:1154, 2022.

[38] S. K. Rai, R. Khanna, A. Avni, and S. Mukhopadhyay. Heterotypic electrostatic interactions control complex phase separation of tau and prion into multiphasic condensates and co-aggregates. *Proc. Natl. Acad. Sci. U.S.A.*, 120:e2216338120, 2023.

[39] J. R. Mann and C. J. Donnelly. RNA modulates physiological and neuropathological protein phase transitions. *Neuron*, 109:2663–2681, 2021.

[40] A. Ishiguro, J. Lu, D. Ozawa, Y. Nagai, and A. Ishihama. Als-linked fus mutations dysregulate g-quadruplex-dependent liquid–liquid phase separation and liquid-to-solid transition. *Chem. Sci.*, 297:101284, 2021.

[41] Z. Liu, S. Zhang, J. Gu, Y. Tong, Y. Li, X. Gui, H. Long, C. Wang, C. Zhao, J. Lu, L. He, Y. Li, Z. Liu, D. Li, and C. Liu. Hsp27 chaperones FUS phase separation under the modulation of stress-induced phosphorylation. *Nature Structural and Molecular Biology*, 27:363–372, 2020.

[42] C. Wang, Y. Duan, G. Duan, Q. Wang, K. Zhang, X. Deng, B. Qian, J. Gu, Z. Ma, S. Zhang, L. Guo, C. Liu, and Y. Fang. Stress induces dynamic, cytotoxicity-antagonizing TDP-43 nuclear bodies via paraspeckle lncRNA NEAT1-mediated liquid-liquid phase separation. *Mol. Cell*, 79:443–458, 2020.

[43] Jinge Gu, Chen Wang, Rirong Hu, Yichen Li, Shengnan Zhang, Yunpeng Sun, Qiangqiang Wang, Dan Li, Yanshan Fang, and Cong Liu. Hsp70 chaperones TDP-43 in dynamic, liquid-like phase and prevents it from amyloid aggregation. *Cell Res.*, 31:1024–1027, 2021.

[44] H. Yu, Shan Lu, Kelsey G., D. Singh, S. Vazquez-Sanchez, O. Tapia, D. Toprani, M. S. Beccari, J. R. Yates, S. Da Cruz, J. M. Newby, M. Lafarga, A. S. Gladfelter, E. Villa, and D. W. Cleveland. HSP70 chaperones RNA-free TDP-43 into anisotropic intranuclear liquid spherical shells. *Science*, 371:eabb4309, 2021.

[45] A. M. Küffner, M Linsenmeier, F. Grigolato, M. Prodan, R. Zuccarini, U. C. Palmiero, L. Faltova, and P. Arosio. Sequestration within biomolecular condensates inhibits Aβ-42 amyloid formation. *Chem. Sci.*, 12:4373–4382, 2021.

[46] W. P. Lipinski, B. S. Visser, I. Robu, M. A. A. Fakhree, S. Lindhoud, M. M. A. E. Claessens, and E. Spruijt. Biomolecular condensates can both accelerate and suppress aggregation of α-synuclein. *Science Advances*, 48:eabq6495, 2022.
$\star$ The study utilized three complex coacervate systems comprising of charged polypeptides, RNA or ATP to study aggregation kinetics of α-synuclein based on its partitioning into these condensates. It was observed that α-synuclein aggregation was accelerated upon localization to the condensate interface when compared to the interior.

[47] X. Dong, S. Bera, Q. Qiao, Y. Tang, Z. Lao, Y. Luo, E. Gazit, and G. Wei. Liquid−liquid phase separation of tau protein is encoded at the monomeric level. *J. Phys. Chem. Lett.*, 12:2576–2586, 2021.

[48] W. Zheng, G. L. Dignon, N. Jovic, X. Xu, R. M. Regy, N. L. Fawzi, Y. C. Kim, R. B. Best, and J. Mittal. Molecular details of protein condensates probed by microsecond long atomistic simulations. *J. Phys. Chem. B*, 124(51):11671–11679, 2020.
$\star\star$ The study presents a pioneering approach to investigate the dynamics and interactions of protein condensates using the phase coexistence method at all-atom system resolution. The authors showed that condensed phase interactions of disordered domains may involve a combination of hydrophobic, hydrogen bond, salt bridge, π–π and cation$-\pi$interactions. It was also revealed that ion partitioning within the condensed phase is determined by the charge distribution of proteins.

[49] L. A Gruijs da Silva, F. Simonetti, S. Hutten, H. Riemenschneider, E. L. Sternburg, L. M. Pietrek, J. Gebel, V. Dötsch, D. Edbauer, G. Hummer, L. S. Stelzl, and D. Dormann. Disease-linked TDP-43 hyperphosphorylation suppresses TDP-43 condensation and aggregation. *EMBO J.*, 41:e108443, 2022.

[50] M. Paloni, R. Bailly, Lu. Ciandrini, and A. Barducci. Unraveling molecular interactions in liquid–liquid phase separation of disordered proteins by atomistic simulations. *J. Phys. Chem. B*, 124(41):9009–9016, 2020.

[51] H. Fatafta, M. Khaled, M. C. Owen, A. Sayyed-Ahmad, and B. Strodel. Amyloid-β peptide dimers undergo a random coil to β-sheet transition in the aqueous phase but not at the neuronal membrane. *Proc. Natl. Acad. Sci. U.S.A.*, 118:e2106210118, 2021.

[52] B. Strodel. Amyloid aggregation simulations: challenges, advances and perspectives. *Curr. Opin. Cell Biol.*, 67:145–152, 2021.

[53] G. L. Dignon, W. Zheng, Y. K. Kim, R. B. Best, and J. Mittal. Sequence determinants of protein phase behavior from a coarse-grained model. *PLoS Comput. Biol.*, 14:1–23, 2018.

[54] G. L. Dignon, W. Zheng, Y. C. Kim, and J. Mittal. Temperature-controlled liquid–liquid phase separation of disordered proteins. *ACS Cent. Sci.*, 5(5):821–830, 2019.

[55] A. Garaizar and J. R. Espinosa. Salt dependent phase behavior of intrinsically disordered proteins from a coarse-grained model with explicit water and ions. *J. Chem. Phys.*, 155(12):125103, 2021.

[56] S. Wohl, M. Jakubowski, and W. Zheng. Salt-dependent conformational changes of intrinsically disordered proteins. *J. Phys. Chem. Lett.*, 12(28):6684–6691, 2021.

[57] T. M. Perdikari, N. Jovic, G. L. Dignon, Y. C. Kim, N. L. Fawzi, and J. Mittal. A predictive coarse-grained model for position-specific effects of post-translational modifications. *Biophys. J.*, 120(7):1187–1197, 2021.

[58] R. M. Regy, G. L. Dignon, W. Zheng, Y. C. Kim, and J. Mittal. Sequence dependent phase separation of protein-polynucleotide mixtures elucidated using molecular simulations. *Nucleic Acids Res.*, 48(22):12593–12603, 2020.

[59] A. P. Latham and B. Zhang. Maximum entropy optimized force field for intrinsically disordered proteins. *J. Chem. Theory Comput.*, 16(1):773–781, 2020.

[60] S. Das, Y.-H. Lin, R. M. Vernon, J. D. Forman-Kay, and H. S. Chan. Comparative roles of charge, π, and hydrophobic interactions in sequence-dependent phase separation of intrinsically disordered proteins. *Proc. Natl. Acad. Sci. U.S.A.*, 117(46):28795–28805, 2020.

[61] T. Dannenhoffer-Lafage and R. B. Best. A data-driven hydrophobicity scale for predicting liquid–liquid phase separation of proteins. *J. Phys. Chem. B*, 125(16):4046–4056, 2021.

[62] G. Tesei, T. K. Schulze, R. Crehuet, and K. Lindorff-Larsen. Accurate model of liquid–liquid phase behavior of intrinsically disordered proteins from optimization of single-chain properties. *Proc. Natl. Acad. Sci. U.S.A.*, 118(44):e2111696118, 2021.

[63] R. M. Regy, J. Thompson, Y. C. Kim, and J. Mittal. Improved coarse-grained model for studying sequence dependent phase separation of disordered proteins. *Protein Sci.*, 30(7):1371–1379, 2021.

[64] J. A. Joseph, A. Reinhardt, A. Aguirre, P. Y. Chew, K. O. Russell, J. R. Espinosa, A. Garaizar, and R. Collepardo-Guevara. Physics-driven coarse-grained model for biomolecular phase separation with near-quantitative accuracy. *Nat. Comput. Sci.*, 1:732–743, 2021.

[65] H. Jafarinia, E. van der Giessen, and P. R. Onck. Phase separation of toxic dipeptide repeat proteins related to C9orf72 ALS/FTD. *Biophys. J.*, 119:843–851, 2020.

[66] C. L. Ren, Y. Shan, P. Zhang, H. M. Ding, and Y. Q. Ma. Uncovering the molecular mechanism for dual effect of ATP on phase separation in FUS solution. *Sci. Adv.*, 8:eabo7885, 2022.

[67] J. A. Joseph, J. R. Espinosa, I. Sanchez-Burgos, A. Garaizar, D. Frenkel, and R. Collepardo-Guevara. Thermodynamics and kinetics of phase separation of protein-RNA mixtures by a minimal model. *Biophys. J.*, 120:1219–1230, 2021.

[68] G. Valdes-Garcia, L. Heo, L. J. Lapidus, and M. Feig. Modeling concentration-dependent phase separation processes involving peptides and RNA via residue-based coarse-graining. *J. Chem. Theory Comput.*, 19(2):669–678, 2023.

[69] C. Her, T. M Phan, N. Jovic, U. Kapoor, B. E. Ackermann, A. Rizuan, Y. C. Kim, J. Mittal, and G. T. Debelouchina. Molecular interactions underlying the phase separation of hp1α: role of phosphorylation, ligand and nucleic acid binding. *Nucleic Acids Res.*, 50(22):12702–12722, 2022.

[70] A. P. Latham and B. Zhang. Unifying coarse-grained force fields for folded and disordered proteins. *Current Opinion in Structural Biology*, 72:63–70, 2022.

[71] A. R. Tejedor, A. Garaizar, J. Ramírez, and J. R. Espinosa. RNA modulation of transport properties and stability in phase-separated condensates. *Biophys. J.*, 12:5169–5186, 2021.

[72] Z. Benayad, S. von B ulow, L. S. Stelzl, and G. Hummer. Simulation of FUS protein condensates with an adapted coarse-grained model. *J. Chem. Theory Comput.*, 17(1):525–537, 2021.

[73] M. Tsanai, P. W. J. M. Frederix, C. F. E. Schroer, P. C. T. Souza, and S. J. Marrink. Coacervate formation studied by explicit solvent coarse-grain molecular dynamics with the Martini model. *Chem. Sci.*, 12:8521–8530, 2021.

[74] N. T. Co, M. S. Li, and P. Krupa. *Computational Models for the Study of Protein Aggregation*, pages 51–78. Springer US, New York, NY, 2022.

[75] G. Bellesia and J.-E. Shea. Self-assembly of β-sheet forming peptides into chiral fibrillar aggregates. *J. Chem. Phys.*, 126:245104, 2007.

[76] A. Magno, R. Pellarin, and A. Caflisch. Mechanisms and kinetics of amyloid aggregation investigated by a phenomenological coarse-grained model. In *Computational modeling of biological systems*, pages 191–214. Springer, 2012.

[77] S. Ranganathan, S. K. Maji, and R. Padinhateeri. Defining a physical basis for diversity in protein self-assemblies using minimal model. *J. Am. Chem. Soc.*, 138:13911–13922, 2016.

[78] B. Szała-Mendyk and A. Molski. Diverse aggregation kinetics predicted by a coarse-grained peptide model. *J. Phys. Chem. B*, 125:7587–7597, 2021.

[79] B. Szała-Mendyk and A. Molski. Side chain geometry determines the fibrillation propensity of a minimal two-beads-per-residue peptide model. *J. Phys. Chem. B*, 126(31):5772–5780, 2022.

[80] H. Xie, A. Rojas, G. G. Maisuradze, and G. Khelashvili. Mechanistic kinetic model reveals how amyloidogenic hydrophobic patches facilitate the amyloid-β fibril elongation. *ACS Chem. Neurosci.*, 13(7):987–1001, 2022.

[81] A. Kumar, D. Chakraborty, M. L. Mugnai, J. E. Straub, and D. Thirumalai. Sequence determines the switch in the fibril forming regions in the low-complexity FUS protein and its variants. *J. Phys. Chem. Lett.*, 12:9026–9032, 2021.

[82] X . Xiao, Y. Wang, D. T. Seroski, K. M. Wong, R. Liu, A. K. Paravastu, G. A. Hudalla, and C. K. Hall. De novo design of peptides that coassemble into βsheet-based nanofibrils. *Sci. Adv.*, 7:eabf7668, 2021.

[83] X. Xiao, A. S. Robang, S. Sarma, J. V. Le, M. E. Helmicki, M. J. Lambert, R. Guerrero-Ferreira, J. Arboleda-Echavarria, A. K. Paravastu, and C. K. Hall. Sequence patterns and signatures: Computational and experimental discovery of amyloid-forming peptides. *Proc. Natl. Acad. Sci. U.S.A. Nexus*, 1(5), 11 2022.
⋆ The study describes a new computational algorithm for the discovery of amyloid-forming petides with desired supramolecular structures. The *pep*tide *a*ssembly *d*esign (PepAD) algorithm was combined with the FoldAmyloid tool and coarse-grained, discontinuous molecular dynamics (DMD) simulations to predict eight 7-mer peptides which formed anti-parallell β-sheets in experiments. Moreover, the authors defined five sequence patterns associated with fibrillation which broadens our understanding of the relationship between peptide sequence and fibril morphology.

[84] A. Michaels, T. C. T. an Šarić, S. Curk, K. Bernfur, P. Arosio, G. Meisl, A. J. Dear, S. I. A. Cohen, M. Dobson, C. M. Vendruscolo, S. Linse, and T. P. J. Knowles. Dynamics of oligomer populations formed during the aggregation of alzheimer's Aβ42 peptide. *Nat. Chem.*, 12:445–451, 2020.

[85] A. J. Dear, G. Meisl, A. Šarić, T. C. T. Michaels, M. Kjaergaard, S. Linse, and T. P. J. Knowles. Identification of on- and off-pathway oligomers in amyloid fibril formation. *Chem. Sci.*, 11:6236–6247, 2020.

[86] T. C. T. Michaels, L. X. Liu, S. Curk, P. G. Bolhuis, A. Šarić, and T. P. J. Knowles. Reaction rate theory for supramolecular kinetics: application to protein aggregation. *Molecular Physics*, 1166:3055–3065, 2018.

[87] S. J. Bunce, Y. Wang, K. L. Stewart, A. E. Ashcroft, S. E. Radford, C. K. Hall, and A. J. Wilson. Molecular insights into the surface-catalyzed secondary nucleation of amyloid-β40 (Aβ40) by the peptide fragment Aβ16-22. *Sci Adv.*, 5:2375–2548, 2019.

[88] A.R. Tejedor, I. Sanchez-Burgos, M. Estevez-Espinosa, A. Garaizar, R. Collepardo-Guevara, J. Ramirez, and J. R. Espinosa. Protein structural transitions critically transform the network connectivity and viscoelasticity of RNA-binding protein condensates but RNA can prevent it. *Nat. Commun.*, 13:5717, 2022.
⋆ The authors used a residue-level CG model coupled with a dynamical algorithm to model the time-dependent formation of inter-protein β-sheets within FUS and hnRNAP1 condensates. The simulations indicate that the formation of β-sheets significantly increases the viscosity of condensates, particularly at low temperatures. Further, they observed that recruitment of high concentrations of RNA into condensates decelerates the accumulation of β-sheets through a combination of attractive RNA-protein interactions and repulsive RNA-RNA interactions. These findings imply a critical role of RNA in regulating the occurrence of pathological aggregation within biomolecular condensates.

[89] S. J. Marrink and D. P. Tieleman. Perspective on the martini model. *Chem. Soc. Rev.*, 42:6801–6822, 2013.

[90] S. Ranganathan and E. Shakhnovich. The physics of liquid-to-solid transitions in multi-domain protein condensates. *Biophys. J.*, 121(14):2751–2766, 2022.

[91] Y. Xing, A. Nandakumar, A. Kakinen, Y. Sun, T. P Davis, C. Ke, and F. Ding. Amyloid aggregation under the lens of liquid−liquid phase separation. *J. Phys. Chem. Lett.*, 12:368–378, 2021.
⋆ The dynamics of droplet-to-fibril conversion was studied for a model CG peptide in a concentration-dependent manner using discrete molecular dynamics (DMD) simulations. The CG peptide model was allowed to adopt two low energy states: fibrillation incompetent (helical or random coil conformations) and fibrillation competent (β-sheet) states. The aggregation kinetics of the CG peptides could be controlled by adjusting the energy barriers of these states. The authors determined the binodal and spinodal concentrations at the low concentration regime and observed that fibrillation via LLPS was only occured at concentrations above the binodal concentration through the formation of a high-density liquid phase (HDLP) comprising of stable (above spinodal concentration) or transient oligomers (below spinodal concentration). Overall, the study provides a unified picture of amyloid formation within the context of LLPS over a wide range of concentrations and is relevant to the etiology of amyloid diseases.

[92] M. Cheon, I. Chang, and C. K. Hall. Extending the prime model for protein aggregation to all 20 amino acids. *Proteins*, 78:2950–2960, 2010.

[93] T. Bereau and M. Deserno. Generic coarse-grained model for protein folding and aggregation. *J. Chem. Phys.*, 130:235106, 2009.

[94] A. Saric, T. C. T. Michaels, A. Zaccone, T. P. J. Knowles, and D. Frenkel. Kinetics of spontaneous filament nucleation via oligomers: Insights from theory and simulation. *J. Chem. Phys.*, 145:211926, 2016.

[95] Y. Xing, N. Andrikopoulos, Z. Zhang, Y. Sun, P. C. Ke, and F. Ding. Modulating nanodroplet formation en route to fibrillization of amyloid peptides with designed flanking sequences. *Biomacromolecules*, 23(10):4179–4191, 2022.

[96] A. Garaizar, J. R. Espinosa, J. A. Joseph, G. Krainer, Y. Shen, T. P.J. Knowles, and R. Collepardo-Guevara. Aging can transform single-component protein condensates into multiphase architectures. *Proc. Natl. Acad. Sci. U.S.A.*, 119(26):e2119800119, 2022.

[97] M. Vendruscolo and M. Fuxreiter. Sequence determinants of the aggregation of proteins within condensates generated by liquid-liquid phase separation. *J. Mol. Model.*, 434:167201, 2022.

[98] T. E. Gartner and A. Jayaraman. Modeling and simulations of polymers: A roadmap. *Macromolecules*, 52:755–786, 2019.

[99] M. Mioduszewski, Ł.and Cieplak. Protein droplets in systems of disordered homopeptides and the amyloid glass phase. *Phys. Chem. Chem. Phys.*,, 22:15592, 2020.

[100] A. Rizuan, N. Jovic, T. M. Phan, Y. C. Kim, and J. Mittal. Developing bonded potentials for a coarse-grained model of intrinsically disordered proteins. *J. Chem. Inf. Model.*, 62(18):4474–4485, 2022.
⋆ The authors present a new coarse-grained computational model, HPS-SS, for simulating the behavior of intrinsically disordered proteins (IDPs). The model uses a dihedral angle potential to capture the transient helical structures of IDPs. The model is parameterized using Cα-based helix assignment rules and helical propensities of 20 amino acids. The results demonstrate that the HPS-SS model is able to accurately reproduce structural features of IDPs, as validated by comparison to α-helicity estimates based on NMR experiments. The model's simplicity also makes it suitable for large-scale assembly simulations.